Neurodegeneration beyond the primary visual pathways in a population with a high incidence of normal-pressure glaucoma

Boucard, Christine C; Hanekamp, Sandra; Curcic-Blake, Branisalava; Ida, Masahiro; Yoshida, Masaki; Cornelissen, Frans W

Published in:
Ophthalmic and physiological optics

DOI:
10.1111/opo.12297

Publication date:
2016

OPO OPHTHALMIC & PHYSIOLOGICAL OPTICS
THE JOURNAL OF THE COLLEGE OF OPTOMETRISTS

Ophthalmic & Physiological Optics ISSN 0275-5408

Neurodegeneration beyond the primary visual pathways in a population with a high incidence of normal-pressure glaucoma

Christine C. Boucard[1,*], Sandra Hanekamp[2,*], Branislava Ćurčić-Blake[3], Masahiro Ida[4], Masaki Yoshida[1,†] and Frans W. Cornelissen[2,†]

[1]Department of Ophthalmology, Jikei University School of Medicine, Tokyo, Japan, [2]Laboratory for Experimental Ophthalmology, University Medical Center Groningen, University of Groningen, The Netherlands, [3]Department of Neuroscience, University of Groningen, University Medical Center Groningen, The Netherlands, and [4]Department of Radiology, Tokyo Metropolitan Health and Medical Treatment Corporation, Ebara Hospital, Tokyo, Japan

Citation information: Boucard CC, Hanekamp S, Ćurčić-Blake B, Ida M, Yoshida M & Cornelissen FW. Neurodegeneration beyond the primary visual pathways in a population with a high incidence of normal-pressure glaucoma. *Ophthalmic Physiol Opt* 2016; 36: 344–353. doi: 10.1111/opo.12297

Keywords: diffusion tensor imaging, glaucoma, magnetic resonance imaging, neurodegeneration, normal-pressure glaucoma

Correspondence: Sandra Hanekamp
E-mail address: sandrahanekamp@gmail.com

*These authors share first authorship.

†These authors share last authorship.

Received: 11 November 2015; Accepted: 7 March 2016

Abstract

Purpose: Glaucoma is the most common age-related neurodegenerative eye disease in western society. It is an insidious disease that, when untreated or detected too late, leads inevitably to blindness. An outstanding issue is whether glaucoma should be considered exclusively an eye disease or also a brain disease. To further examine it, we used Diffusion Tensor Imaging (DTI) to study white matter integrity in a Japanese glaucoma population. This population has a very high incidence of normal-pressure glaucoma, in which optic nerve damage occurs in the absence of the elevated eye pressure that characterises the more common form of glaucoma.

Methods: We performed DTI in 30 participants with normal-pressure glaucoma and 21 age-matched healthy controls. We used voxel-wise tract-based spatial statistics to compare fractional anisotropy and mean diffusivity of the white matter of the brain between patients and control group. Whole-brain and region of interest-based analyses served to find associations between diffusion indices and clinical measures of glaucomatous damage.

Results: Fractional Anisotropy was significantly lower in glaucoma patients in a cluster in the right occipital lobe ($p < 0.05$; family-wise error-corrected) comprising fibres of both the optic radiation and the forceps major. Additional analysis confirmed bilateral involvement of the optic radiations and forceps major and additionally revealed damage to the corpus callosum and parietal lobe ($p < 0.09$; family-wise error-corrected). The region of interest-based analysis revealed a positive association between Fractional Anisotropy of the optic radiation and optic nerve damage.

Conclusions: In this specific population, glaucoma is associated with lower Fractional Anisotropy in the optic radiations, forceps major and corpus callosum. We interpret these reductions as evidence for white matter degeneration in these loci. In particular, the degeneration of the corpus callosum suggests the presence of neurodegeneration of the brain beyond what can be explained on the basis of propagated retinal and pre-geniculate damage. We discuss how this finding links to the emerging view that a brain component that is independent from the eye damage plays a role in the aetiology of glaucoma.

Introduction

Glaucoma is the most common age-related neurodegenerative eye disease in western society and one of the four major blinding eye diseases.[a] Glaucoma is an insidious disease that leads to peripheral visual field loss and when untreated or detected too late, inevitably leads to blindness, resulting in a profound loss of quality of life for the individual and his family and in major costs to society.

The classic view of glaucoma[b] is that of an eye disease in which elevated intraocular pressure (IOP) mechanically damages the optic nerve (ON) causing the death of retinal ganglion cells (RGCs). Indeed, in high-pressure glaucoma (HPG, the most common form of glaucoma), RGC and ON damage are associated with an elevated IOP (>21 mmHg).[1] However, this view cannot be complete as glaucoma with normal levels of IOP is commonly reported as well. In such normal-pressure glaucoma (NPG), damage occurs to the ON without the eye pressure exceeding the normal range. By definition, NPG only differs from HPG in that the IOP is consistently below 22 mmHG.[1] Moreover, rather than being a disease restricted to the eye, damage of the RCGs extends to the axons that form the primary visual pathways.[c] Previous studies have shown alterations along the entire length of the primary visual pathways in both the grey and white matter (WM).[2–14] In conformation, a recent meta-analysis of diffusion tensor imaging (DTI) studies found that glaucoma is associated with lower fractional anisotropy (FA) in the ON and optic radiation (OR), as well as with an increased mean diffusivity as determined by DTI in the optic tracts.[15] In particular, involvement of post-geniculate structures begs the question whether glaucoma should be considered a brain disease as well. However, most post-geniculate primary visual pathway damage can be relatively straightforwardly explained as a consequence of propagated retinal and ON (i.e. pre-geniculate) damage – either through Wallerian degeneration or anterograde transsynaptic degeneration (ATD).

However, research to date has tended to focus on brain involvement in patients with HPG.[2–5,7–10,12,14–21] In contrast, systematic research into neuroanatomical changes associated with NPG is scarce.[11,18] This may limit our understanding of glaucoma in general, as HPG and NPG may be the two sides of the same coin. Hence, studying NPG may reveal different properties of the mechanism underlying glaucoma. In our present study, we examine WM integrity in a Japanese glaucoma population using tract-based spatial statistics (TBSS). In this population, over 90% of glaucoma patients have NPG.[22] First of all, we expect changes in the structural properties in WM of the primary visual pathways in patients compared to age-matched healthy controls. Second, we expect to find associations between these changes and clinical measures that assess glaucomatous damage. Additionally, if we were to find changes in WM structures beyond those that can be considered a consequence of propagated ON damage, this would be an important indication that there is an independent brain component to glaucoma.

Methods

Subjects

Thirty participants diagnosed with primary open-angle glaucoma were recruited among the ophthalmologic patient population of the Jikei University hospital (Tokyo, Japan). The diagnosis of glaucoma required examination of the head of the ON through Optical Coherence Tomography (OCT) as well as a visual field exploration. All participants presented an IOP below 21 mmHg. The mean age of the glaucoma group was 52.0 (S.D. = 10.7) years. The control group included 21 healthy participants with no history of glaucoma or other neurological problems. The mean age of the control group was 52.3 (S.D. = 15.3) years. This study conformed to the tenets of the Declaration of Helsinki and was approved by the medical ethical committee of the Jikei University School of Medicine. All participants gave their informed written consent prior to participation.

Table 1. Patients' characteristics

	Glaucoma (*N* = 30) Mean (S.D.)	Healthy controls (*N* = 21) Mean (S.D.)	*p*-Value
Age	52.0 (10.7)	52.3 (15.3)	0.89
Male sex, %	77%	48%	0.033
MD-HFA			
Right eye	−8.9 (9.4)	0.9 (1.3)	<0.0001
Left eye	−6.8 (8.9)	0.4 (1.3)	<0.0001
RNFLT			
Right eye	66.9 (17.8)	100.0 (17.4)	<0.0001
Left eye	69.3 (15.4)	101.8 (12.8)	0.005

MD-HFA, mean deviation (dB); RNFLT, retinal nerve fibre layer thickness (micron); S.D., standard deviation.

[a]These four being: cataract, macular degeneration, glaucoma and diabetic retinopathy.

[b]We refer here to primary open-angle glaucoma (POAG): chronic, progressive optic neuropathies that have in common characteristic morphological changes at the optic nerve head and retinal nerve fiber layer in the absence of other ocular disease or congenital anomalies.

[c]We define the primary visual pathways as consisting of the retina, optic nerve (ON), optic chiasm, optic tract, lateral geniculate nucleus (LGN), optic radiation (OR), and the visual cortex. Secondary visual pathways would comprise connections between visual cortical areas, including those in the corpus callosum. The anterior visual pathway refers to structures before the LGN (i.e. pre-geniculate structures), whereas the posterior visual pathway refers to structures after this nucleus (i.e. post-geniculate structures).

Clinical data

The clinical data for each participant can be found in *Table 1*.

Retinal nerve fibre layer thickness (RNFLT) was measured by means of OCT (Stratus OCT 3000; Carl Zeiss Meditec, Dublin, CA, USA). The average values (average in micron) in the glaucoma group were 66.9 (S.D. = 17.8) for the right eye and 69.3 (S.D. = 15.4) for the left eye. The OCT values in the control group were 100.0 (S.D. = 17.4) for the right eye and 101.8 (S.D. = 12.8) for the left eye.

Visual field sensitivity (expressed as mean deviation: MD) was measured using the 30-2 program SITA (Swedish Interactive Threshold Algorithm) standard of Humphrey Field Analyser (HFA) (Carl Zeiss Meditec). MD-HFA values correspond to the weighted average in visual field sensitivity relative to the norm for a particular age group. In the glaucoma group, the mean MD-HFA values were −8.9 (S.D. = 9.4) for the right eye and −6.8 (S.D. = 8.9) for the left eye. As expected, the MD-HFA values of the control group did not significantly vary from 0. The mean MD-HFA values were 0.9 (S.D. = 1.3) for the right eye and 0.4 (S.D. = 1.3) for the left eye.

Neuro-imaging

Whole brain high-resolution MRI was performed on a Siemens 3 Tesla MAGNETOM Trio A Tim System (Siemens, Erlangen, Germany) with a 32 channels matrix head coil.

The anatomical scan was acquired with a T1 weighted 3D MPRAGE sequence: 9 degrees flip angle, TR 2300 ms, TE 2.98 ms, matrix size 256 × 256, field of view 256, 176 slices with a voxel size of $1 \times 1 \times 1$ mm^3. The brain images were corrected for intensity inhomogeneity using the built-in console.

The DTI data of the whole brain were acquired using a single shot echo planar sequence collected with 64 directions of motion proving gradient and including an additional b0 image. The scanning parameters were: TR 8800 ms, TE 87 ms, field of view 210–230, 140 × 140 matrix, slice distance factor 5%, voxel size $1.5 \times 1.5 \times 1.5$ mm, b value 1000 s mm^{-2}. The data were acquired with an acceleration factor of 2 (GRAPPA).

Group analysis: tract-based spatial statistics (TBSS)

Group analysis of the FA and MD-DTI data was carried out using automated voxel-wise tract-based spatial statistics (TBSS) implemented in FMRIB Software Library.[23]

The TBSS method consisted in first correcting the data for the effects of head movement and eddy currents. FA images were created by fitting a tensor model to the raw diffusion data using FMRIB's Diffusion Toolbox (part of FMRIB Software Library). Second, using non-linear registration, the FA images were aligned to a standard space (FMRIB58_FA). Third, a mean FA image as well as a mean FA skeleton representing the centres of all tracts common to the group was created. The resulting 'mean FA skeleton' was then thresholded to a mean FA of 0.25 to suppress areas of low mean FA and/or high inter-subject variability and exclude minor tracts carrying high inter-subject variability and/or partial volume effects. Finally, each subject's aligned FA data was projected onto the 'mean FA skeleton'. Basically, each voxel contained in the 'mean FA skeleton' took the subject's FA value from the local centre of the nearest relevant tract, reducing potential problems related to alignment and smoothing. To compare MD-DTI values, FA images were used to achieve the non-linear registration and skeletonisation stages, and to estimate the projection vectors from each individual subject onto the mean FA skeleton. The nonlinear warps and skeleton projection were then applied to MD-DTI.

We used FMRIB Software Library's randomise permutation test with a threshold-free cluster-enhancement (TFCE) correction for multiple comparisons ($p < 0.05$) to statistically compare the glaucoma and control groups' FA and MD-DTI values included in the 'mean FA skeleton'. The number of permutations was set to 2000. Considering glaucoma is an age-related disease, we included age as a covariate in our analysis. To check whether gender could also be a confounder, we compared FA values between females and males using FMRIB Software Library's randomise permutation test (number of permutations was set to 2000) with a TFCE correction for multiple comparisons ($p < 0.05$).

Exploratory tract-based spatial statistics (TBSS) analysis

An exploratory data analysis was performed to gain more insight in the causes of WM changes revealed by our initial TBSS analysis. For this purpose, the results of the whole-brain analysis with a TFCE correction for multiple comparisons were examined using a more lenient statistical threshold of $p < 0.09$.

Region of Interest (ROI)-based multiple regression analysis

In order to assess associations between WM integrity and clinical measures of glaucomatous damage (RNFLT and MD-HFA) we performed a ROI-based analysis using a multiple regression with TFCE correction for multiple comparisons. We anticipated neurodegeneration in the left and right OR.[15] The OR ROI was taken from the Juelich Histological Atlas. ROIs were multiplied with the skeletonized FA image using *fslmaths* resulting in

masks specific to our participants. Clinical measures were de-meaned and added to the analysis as covariates. Considering glaucoma is an age-related disease, we corrected for age. We used FMRIB Software Library's randomise permutation test with a TFCE correction for multiple comparisons ($p < 0.05$). The number of permutations was set to 2000.

Additional *post-hoc* ROI-based analyses were performed to verify whether neurodegeneration in unanticipated WM structures was associated with clinical measures.

Exploratory whole-brain multiple regression analysis

To further explore the relationship between the diffusion indices (FA and MD-DTI) and the clinical measures (RNFLT and MD-HFA), a whole-brain multiple regression analysis was performed. The clinical measures were all de-meaned and added to the multiple regression analysis as covariates. We corrected for age. The significance threshold was set at $p < 0.05$, based on the TFCE statistic image. The number of permutations was set to 2000.

Table 2. Brain region of the main cluster with significant difference between patients with glaucoma and healthy controls corrected with TFCE, cluster size, the *z*-value of the peak in the cluster and its MNI coordinates. Brain regions are identified according to the Juelich Histological Atlas using FMRIB Software Library

Brain region	*MAX* z-statistic	Cluster size (mm^3)	MNI coordinates		
			x	*y*	*z*
57% Optic radiation R, 30% Callosal body	0.986	380	27	−76	2

Results

Demographic and clinical characteristics

The glaucoma and the control groups' demographic and clinical characteristics are summarized in *Table* 1. The groups did not differ in mean age. The gender distribution differed between groups. Of the glaucoma measures, both the RNFLT and the MD-HFA differed between the two groups.

TBSS analysis

In order to assess WM integrity, the FA and MD-DTI values of the two groups were compared using a threshold-free cluster enhancement (TFCE) correction for multiple comparisons. We did not find significant differences in MD-DTI. FA values were significantly lower ($p < 0.05$) in patients with glaucoma compared to healthy controls in a cluster (380 voxels) in the right occipital lobe (*Table 2*). As shown in *Figure 1*, the voxels of this cluster comprise both fibres of the OR as well as fibres of the forceps major (FM;

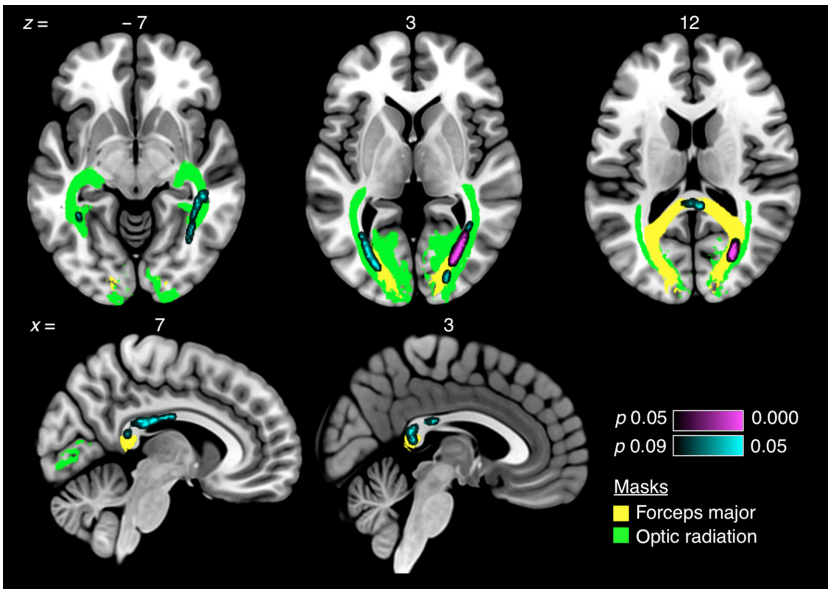

Figure 1. Differences in FA in the white matter of glaucoma patients and controls. White matter region of 380 voxels showing significant difference in fractional anisotropy in three axial slices and two sagittal slices by using a TFCE correction for multiple comparisons. Violet-coloured highlights ($p < 0.05$) and cyan-coloured highlights ($p < 0.09$) show areas with decreased FA in patients with glaucoma compared to healthy controls. For visualization purposes, green-coloured highlights show the fibres of the *optic radiation* and yellow-coloured highlights show the fibres of the *forceps major*.

identified as callosal body using FMRIB Software Library's Juelich Histological Atlas) and could not be exclusively assigned to either one of these fibre tracts. A permutation test revealed that FA values did not differ significantly between genders indicating gender was not a confounding effect.

Explorative TBSS analysis

For two reasons, an additional explorative TBSS analysis using a more lenient statistical threshold ($p < 0.09$) was performed. First, it might help in assigning the FA reduction to the OR, the FM, or both. Second, we wanted to determine if the FA reduction in the glaucoma patients was uni- or bilateral (as would *a priori* be expected). This new analysis revealed that the previously identified cluster in the right occipital lobe increased to 823 voxels and contained both fibres of the right OR as well as the right FM. In addition, clusters of lower FA values in glaucoma patients appeared in the left occipital lobe, right superior parietal lobe (SPL), and in the body and splenium of the corpus callosum (CC). Similar to the cluster in the right occipital lobe, the left cluster contained fibres of both the OR and FM. (*Table 3; Figure 1).*

ROI-based multiple regression analysis

Figure 2 and *Table 4* show that bilateral in the OR, we found sections that showed a positive relationship between FA values and RNFLT. Such a relationship was not found for FA and HFA-MD. In addition, based upon us finding lower FA in the body and splenium of the corpus callosum in the group-based comparison, we created ROIs of these structures using the ICBM-DTI-81 white-matter labels atlas.[24] In these ROIs, we found no relationship between FA and either of the clinical measures.

Exploratory whole-brain multiple regression analysis

No significant associations were found between the diffusion indices (FA and DTI-MD) and the clinical measures (RNFLT and HFA-MD).

Table 3. Brain regions with significant differences between patients with glaucoma and healthy controls with a more lenient threshold of 0.91 corrected with TFCE, cluster size, the *z*-value of the peak in the cluster and its MNI coordinates. Brain regions are identified according to the Juelich Histological Atlas using FMRIB Software Library

Brain Region	*MAX* z-statistic	Cluster size (mm^3)	MNI Coordinates		
			x	*y*	*z*
57% Optic radiation R, 30% Callosal body	0.986	823	27	−76	2
40% Optic radiation L, 33% Callosal body	0.923	221	−26	−78	2
96% Callosal body	0.919	205	5	−28	22
2% Anterior intra-parietal sulcus R (SPL)	0.923	84	21	−52	42
72% Optic radiation R	0.929	69	22	−87	4
95% Callosal body	0.915	60	6	−41	15
70% Callosal body	0.916	43	−13	−34	24
44% Optic radiation L, 40% Callosal body	0.919	43	−37	−49	−5
79% Callosal body	0.914	19	2	−38	10

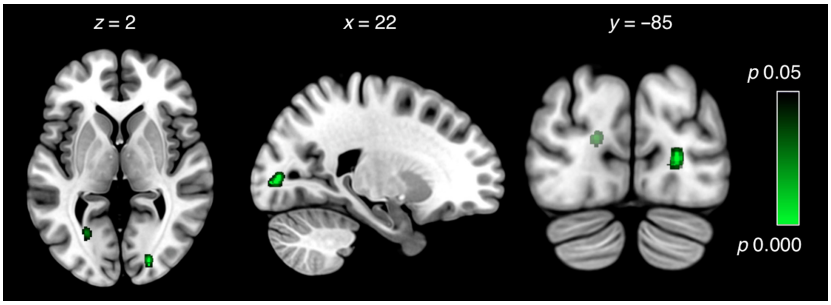

Figure 2. Regions of the optic radiations showing a relation between FA and RNFLT. Results are based on a ROI-based multiple regression analysis that included glaucoma patients and controls. Representative axial, sagittal, and coronal slices show the white matter regions of the OR for which the analyses revealed a significant relationship between FA and RNFLT values ($p < 0.05$; family-wise error-corrected).

Table 4. Clusters of the optic radiation with a significant difference showing an association between FA and RNFLT. Results are based on a ROI-based multiple regression analysis that included glaucoma patients and controls corrected with TFCE ($p < 0.05$), cluster size, the *z*-value of the peak in the cluster and its MNI coordinates. Brain regions are identified according to the Juelich Histological Atlas using FMRIB Software Library

Brain Region	*MAX* z-statistic	Cluster size (mm^3)	MNI Coordinates		
			x	*y*	*z*
72% Optic radiation R	0.973	31	22	−85	5
56% Optic radiation L	0.964	15	−16	−88	13
39% Optic radiation L, 22% Callosal body	0.964	12	−24	−67	0
8% Optic radiation L	0.97	9	−34	−51	−12

Discussion

The current study shows lower FA values in a number of clusters in the occipital lobes of glaucoma patients compared to healthy controls. We interpret lower FA values as evidence for neurodegeneration. The clusters comprise fibres of the OR, FM and the body and splenium of the CC. Furthermore, we found a positive association between FA and RNFLT for the bilateral ORs. What we consider our most remarkable finding is the evidence for degeneration of the body and the splenium of the CC. As we will discuss below in more detail, this latter finding in particular indicates degeneration beyond what can be explained straightforwardly as a propagated consequence of pre-geniculate damage. In our view, this implies the involvement of an independent brain factor in glaucoma.

Neurodegeneration of the optic radiations is consistent with anterograde transsynaptic degeneration *(ATD)*

Both the group and the ROI analysis indicated degeneration of the OR in this specific population. This result corroborates the conclusions of a previous meta-analysis of DTI studies.[3–5,8–11,14] Given that glaucoma is typically considered an eye disease, neurodegeneration of the OR remains a remarkable finding. Two processes could be responsible for it.[25,26] Firstly, via Wallerian degeneration, the breakdown of axons and their accompanying myelin sheaths of the ON could spread 'downstream' along the visual pathways to the LGN. This would result in degeneration of LGN neurons and their axons in the OR. Secondly, due to a decrease of visual input, ATD would cause degeneration of the postsynaptic neuron that is associated with a similar function as the presynaptic neuron (i.e. the 'use it or lose it' principle). On the basis of our present results, we cannot distinguish conclusively between these two explanations. However, there are a number of reasons to assume that ATD is the primary cause of OR degeneration. Firstly, as visual pathway degeneration has been described in very different eye diseases, we have previously argued that the most parsimonious explanation is loss of visual input and subsequent deprivation.[25] Secondly, Wallerian degeneration would predict finding degeneration of the anterior visual pathways (optic chiasm and optic tracts) as well, which we did not. It may be that the OR is more susceptible to damage than other WM structures. For instance, axon size is an important determinant of susceptibility to damage.[27] Us not finding anterior visual pathway degeneration could also be due to challenges in imaging and analysing these relatively small tracts (see also limitations). Thirdly, the neurodegeneration in the right occipital lobe was larger than in the left occipital lobe. Even though the origin of this lateralization remains unknown, it is consistent with the results of the already mentioned DTI meta-analysis.[15] The lateralization might be a consequence of an asymmetry in the –average– location of the visual field defects[9] or be related to a hemispheric functional asymmetry in visual information processing. Either way, lateralization is consistent with OR degeneration being the result of ATD.

Neurodegeneration of the FM, CC, and SPL indicates degeneration beyond the primary visual pathways

The main clusters of degeneration in the occipital lobes (i.e. those near the OR) also contain fibres of the FM. The FM is an interhemispheric fibre bundle that connects the occipital lobes and extends through the splenium of the CC. Here, we also found evidence for neurodegeneration in the glaucoma patients. The FM is thought to be involved in higher-order visual functions such as reading, pattern discrimination, perceptual equivalence, and binocular rivalry.[28] The SPL is involved in visual spatial orientation; degeneration in this lobe could be due to altered viewing behaviour as a consequence of visual field defects. It seems unlikely that the degeneration of the FM, CC, and SPL is a direct consequence of propagated pre-geniculate degeneration, as these structures lie not adjacent to the anterior visual pathways. However, the damage of the OR fibres may locally spreads towards neighbouring axons via Wallerian degeneration.[29] In addition, reduced activity in the primary visual pathways may have downstream effects on vision related regions connected to these pathways, such as the FM. However, while this may explain degeneration of the FM, this does not explain the involvement of the body of the CC.

Neurodegeneration of the CC implicates an independent brain component in glaucoma

In various neurologic diseases, measurement of the CC has been used to assess neuronal degeneration. Therefore, finding neurodegeneration of both the body and splenium of the CC suggests that there may be an additional degenerative mechanism acting in glaucoma. In line with this idea, a study by Ong *et al.*[30] found that – based on manual measurements – the body and genu of the CC where thinner in NPG patients compared to healthy controls. Ong *et al.* suggested that – as the thickness of both the neuroretinal rim area and the CC reflect the number of nerve fibres – the thinning of the CC might have a similar origin as the thinning of the retinal nerve fibre layer (RNFL). On this basis, Ong *et al.* suggested that glaucoma might entail a form of accelerated aging of the central nervous system. However, somewhat countering this specific explanation, the pattern of neurodegeneration seen in glaucoma (i.e. of the visual pathways) is different from that seen in normal aging: in normal aging, the prefrontal cortex is most affected while the visual cortex is mostly spared.[31] To our knowledge, beyond our present results and the study of Ong *et al.*[30], there is no further literature that directly implicates the CC in glaucoma.

A different line of evidence for a brain component to glaucoma comes from recent studies that suggest that glaucoma and Alzheimer's disease share the same underlying pathologic mechanism.[32–35] Glaucoma and Alzheimer's disease are both neurodegenerative, progressive, chronic and age-related diseases and cause RCG degeneration and irreversible neuronal cell loss. In this context, it is rather interesting that our observed pattern of WM degeneration in the CC is also seen in posterior cortical atrophy (PCA), also referred to as 'the visual variant of Alzheimer's disease '.[36–38] PCA is characterized by atrophy of the occipito-temporal (ventral stream) and occipito-parietal (dorsal stream) cortex resulting in both visuospatial and visuoperceptual problems.[39] Secondary degeneration of the splenium has been suggested as one of the characteristics of PCA.[40] Similarly, glaucoma shows a large degree of genetic overlap with Parkinson's disease, another age-related neurodegenerative disease.[34]

Finally, recent studies suggest that the trans-lamina cribrosa pressure difference (the difference between IOP and intracranial pressure) correlates stronger with glaucoma than only IOP.[41–44] Possibly, an abnormal intracranial pressure in glaucoma may somehow also affect the integrity of the CC, since the lower surface of CC forms the roof of the lateral ventricle, which supports the circulation of cerebrospinal fluid. While these lines of evidence do not necessarily converge on the same underlying mechanism, they all support the notion that degeneration of the CC implies a role for an independent brain component in glaucoma. We consider the absence of an association between FA of the CC and RNFLT to be in support of this notion.

Implications

Our study has several implications. First, it challenges the notion that the brain degeneration commonly observed in glaucoma is solely a consequence of propagated pre-geniculate damage. Previous studies suggest that elevated IOP causes the loss and apoptosis of RGCs.[10,45,46] Increased IOP would block the transport of neurotrophic factors (e.g. proteins that regulate the growth, differentiation, and death of neurons), which results in RCG apoptosis and subsequently myelin breakdown or neurodegeneration.[47] Second, our study has revealed a different pattern of WM damage in NPG than the pattern previously described for HPG. This implies that HPG and NPG each have a unique profile of neuronal cell death. The most parsimonious explanation for this is that HPG and NPG each reveal different aspects of one and the same disease that has both an ocular and a brain component to it.

Third, despite the absence of increased IOP, WM integrity is affected in the primary visual pathway and even beyond. The current treatment strategy is lowering IOP, even in NPG.[48] Our study contributes to the idea that neuroprotective medication could be prescribed to prevent degeneration of the primary visual pathways and other brain structures, in addition to the standard treatment that is aimed at normalizing IOP.[49–53]

Limitations

A limitation (shared by all DTI studies) is that a reduction in FA cannot be straightforwardly interpreted as a reduction in WM. Although we interpret FA changes in terms of neurodegeneration, strictly speaking we cannot. Values of the fractional anisotropy (FA) are a quantification of the directionality of water diffusion[54,55] within a voxel. When it is not constrained, as in cerebrospinal fluid or grey matter, water diffuses equally or isotropically in all directions, resulting in lower FA values. Water restricted to the myelinated microstructure of the WM flows parallel to the axonal fibres and becomes anisotropic resulting in higher FA values. A change in FA is thought to reflect microstructural changes in WM. However, lower FA values could also indicate regions of crossing fibres from two fibre populations of similar density (i.e. 'kissing' fibres).[56]

We found no evidence of degeneration in the ON, optic chiasm, and optic tracts. A reason might be that imaging these relatively small structures with DTI is challenging. They are surrounded by cerebrospinal fluid and nearby bony structures and sinus cavities filled with air.[57] In

addition, the ON is prone to motion because of eye movements. Therefore, not finding changes in these structures could be due to an inability to detect these.

The degeneration of the CC was found after applying a more liberal statistical threshold. As such, somewhat more caution than usual must be applied, as the chance for false positive findings increases with a more liberal statistical threshold.

Conclusion

This study investigated WM integrity in a Japanese glaucoma population. This population has a very high incidence of NPG, a sub-class of glaucoma in which ON damage occurs in the absence of elevated IOP. Therefore, our finding of visual pathway degeneration in this population challenges the notion that the elevated IOP is solely responsible for RGC death and subsequent neurodegeneration at the level of the visual pathways.

Most remarkably, in this population, neurodegeneration is not limited to the primary visual pathways, but includes the CC. In our view, this finding is hard to exclusively reconcile with propagated pre-geniculate neurodegeneration thus implying a brain component to glaucoma. Hence, our results suggest that NPG has a different profile of neuronal cell death than HPG. Further research is required to establish whether the neurodegeneration in NPG and HPG is caused by the same or by different mechanisms.

Acknowledgements

CCB was supported by a grant from the Japan Society for the Promotion of Science (JSPS) Postdoctoral Fellowship for Overseas Researchers. SH was supported via FWC by research grants from the Stichting MD Fonds, Landelijke Stichting voor Blinden en Slechtzienden (LSBS), and Algemene Nederlandse Vereniging ter Voorkoming van Blindheid (ANVVB) via UitZicht. BCB was supported by NWO VICI grant (No. 453-11-004) awarded to A. Aleman. The funding organizations had no role in the design or conduct of this research.

References

1. European Glaucoma Society. *Terminology and Guidelines for Glaucoma. European Glaucoma Society*. Savona, Italy: European Glaucoma Society, 2003.
2. Boucard CC *et al.* Changes in cortical grey matter density associated with long-standing retinal visual field defects. *Brain* 2009; 132: 1898–1906.
3. Chang ST *et al.* Optic nerve diffusion tensor imaging parameters and their correlation with optic disc topography and disease severity in adult glaucoma patients and controls. *J Glaucoma* 2014; 23(8): 513–520.
4. Dai H *et al.* Whole-brain voxel-based analysis of diffusion tensor MRI parameters in patients with primary open angle glaucoma and correlation with clinical glaucoma stage. *Neuroradiology* 2013; 55: 233–243.
5. Garaci FG *et al.* Optic nerve and optic radiation neurodegeneration in patients with glaucoma: in vivo analysis with 3-T diffusion-tensor MR imaging. *Radiology* 2009; 252: 496–501.
6. Gupta N, Ang L-C, Noël de Tilly L, Bidaisee L & Yücel YH. Human glaucoma and neural degeneration in intracranial optic nerve, lateral geniculate nucleus, and visual cortex. *Br J Ophthalmol* 2006; 90: 674–678.
7. Hernowo AT, Boucard CC, Jansonius NM, Hooymans JMM & Cornelissen FW. Automated morphometry of the visual pathway in primary open-angle glaucoma. *Invest Ophthalmol Vis Sci* 2011; 52: 2758–2766.
8. Liu T *et al.* Reduced white matter integrity in primary open-angle glaucoma: a DTI study using tract-based spatial statistics. *J Neuroradiol* 2012; 40: 89–93.
9. Murai H *et al.* Positive correlation between the degree of visual field defect and optic radiation damage in glaucoma patients. *Jpn J Ophthalmol* 2013; 57: 257–262.
10. Wang M-Y *et al.* Quantitative 3-T diffusion tensor imaging in detecting optic nerve degeneration in patients with glaucoma: association with retinal nerve fiber layer thickness and clinical severity. *Neuroradiology* 2013; 55: 493–498.
11. Zhang YQ *et al.* Anterior visual pathway assessment by magnetic resonance imaging in normal-pressure glaucoma. *Acta Ophthalmol* 2012; 90: E295–E302.
12. Zikou AK *et al.* Voxel-based morphometry and diffusion tensor imaging of the optic pathway in primary open-angle glaucoma: a preliminary study. *AJNR Am J Neuroradiol* 2012; 33: 128–134.
13. Chen WW *et al.* Structural brain abnormalities in patients with primary open-angle glaucoma: a study with 3T MR imaging. *Invest Ophthalmol Vis Sci* 2013; 54: 545–554.
14. Chen Z *et al.* Diffusion tensor magnetic resonance imaging reveals visual pathway damage that correlates with clinical severity in glaucoma. *Clin Exp Ophthalmol* 2013; 41: 43–49.
15. Li K *et al.* Alteration of fractional anisotropy and mean diffusivity in glaucoma: novel results of a meta-analysis of diffusion tensor imaging studies. *PLoS ONE* 2014; 9: e97445.
16. Gupta N *et al.* Atrophy of the lateral geniculate nucleus in human glaucoma detected by magnetic resonance imaging. *Br J Ophthalmol* 2009; 93: 56–60.
17. Iwata F *et al.* Association of visual field, cup-disc ratio, and magnetic resonance imaging of optic chiasm. *Arch Ophthalmol* 1997; 115: 729–732.
18. Kashiwagi K, Okubo T & Tsukahara S. Association of magnetic resonance imaging of anterior optic pathway with glaucomatous visual field damage and optic disc cupping. *J Glaucoma* 2004; 13: 189–195.

19. Li C *et al.* Voxel-based morphometry of the visual-related cortex in primary open angle glaucoma. *Curr Eye Res* 2012; 37: 794–802.
20. Williams AL *et al.* Evidence for widespread structural brain changes in glaucoma: a preliminary voxel-based MRI study. *Invest Ophthalmol Vis Sci* 2013; 54: 5880–5887.
21. Kitsos G, Zikou AK, Bagli E, Kosta P & Argyropoulou MI. Conventional MRI and magnetisation transfer imaging of the brain and optic pathway in primary open-angle glaucoma. *Br J Radiol* 2009; 82: 896–900.
22. Iwase A *et al.* The prevalence of primary open-angle glaucoma in Japanese: the Tajimi Study. *Ophthalmology* 2004; 111: 1641–1648.
23. Smith SM *et al.* Tract-based spatial statistics: voxelwise analysis of multi-subject diffusion data. *NeuroImage* 2006; 31: 1487–1505.
24. Mori S *et al.* Stereotaxic white matter atlas based on diffusion tensor imaging in an ICBM template. *NeuroImage* 2008; 40: 570–582.
25. Prins D, Hanekamp S & Cornelissen FW. Structural brain MRI studies in eye diseases: are they clinically relevant? A review of current findings *Acta Ophthalmol* 2015; 94(2): 113–21.
26. Raz N, Bick AS, Ben-Hur T & Levin N. Focal demyelinative damage and neighboring white matter integrity: an optic neuritis study. *Mult Scler* 2015; 21: 562–571.
27. Evangelou N *et al.* Size-selective neuronal changes in the anterior optic pathways suggest a differential susceptibility to injury in multiple sclerosis. *Brain* 2001; 124: 1813–1820.
28. Berlucchi G. Visual interhemispheric communication and callosal connections of the occipital lobes. *Cortex* 2014; 56: 1–13.
29. Nucci C *et al.* Brain involvement in glaucoma : advanced neuroimaging for understanding and monitoring a new target for therapy. *Curr Opin Pharmacol* 2013; 13: 128–133.
30. Ong K, Farinelli A, Billson F, Houang M & Stern M. Comparative study of brain magnetic resonance imaging findings in patients with low-tension glaucoma and control subjects. *Ophthalmology* 1995; 102: 1632–1638.
31. Peters R. Ageing and the brain. *Postgrad Med J* 2006; 82: 84–88.
32. Ghiso JA, Doudevski I, Ritch R & Rostagno AA. Alzheimer's disease and glaucoma: mechanistic similarities and differences. *J Glaucoma* 2013; 22(Suppl. 5): S36–S38.
33. Inoue T, Kawaji T & Tanihara H. Elevated levels of multiple biomarkers of Alzheimer's disease in the aqueous humor of eyes with open-angle glaucoma. *Invest Ophthalmol Vis Sci* 2013; 54: 5353–5358.
34. Janssen SF *et al.* The vast complexity of primary open angle glaucoma: disease genes, risks, molecular mechanisms and pathobiology. *Prog Retin Eye Res* 2013; 37: 31–67.
35. Sivak JM. The aging eye: common degenerative mechanisms between the Alzheimer's brain and retinal disease. *Invest Ophthalmol Vis Sci* 2013; 54: 871–880.
36. Levine DN, Lee JM & Fisher CM. The visual variant of Alzheimer's disease: a clinicopathologic case study. *Neurology* 1993; 43: 305–313.
37. Bokde AL *et al.* The effect of brain atrophy on cerebral hypometabolism in the visual variant of Alzheimer disease. *Arch Neurol* 2001; 58: 480–486.
38. Lee AG & Martin CO. Neuro-ophthalmic findings in the visual variant of Alzheimer's disease. *Ophthalmology* 2004; 111: 376–380.
39. Crutch SJ *et al.* Posterior cortical atrophy. *Lancet Neurol* 2012; 11: 170–178.
40. Yoshida T, Shiga K, Yoshikawa K, Yamada K & Nakagawa M. White matter loss in the splenium of the corpus callosum in a case of posterior cortical atrophy: a diffusion tensor imaging study. *Eur Neurol* 2004; 52: 77–81.
41. Jonas JB *et al.* Estimated trans-lamina cribrosa pressure difference versus intraocular pressure as biomarker for open-angle glaucoma. The Beijing Eye Study 2011. *Acta Ophthalmol* 2015; 93(1): e7–e13.
42. Wostyn P *et al.* Intracranial pressure fluctuations: a potential risk factor for glaucoma? *Acta Ophthalmol* 2013; 93(1): e83–4.
43. Zhang Z *et al.* Valsalva manoeuver, intra-ocular pressure, cerebrospinal fluid pressure, optic disc topography: beijing intracranial and intra-ocular pressure study. *Acta Ophthalmol* 2014; 92: e475–e480.
44. Wang YX *et al.* Parapapillary atrophy in patients with intracranial tumours. *Acta Ophthalmol* 2013; 91: 521–525.
45. Sidek S *et al.* Glaucoma severity affects diffusion tensor imaging (DTI) parameters of the optic nerve and optic radiation. *Eur J Radiol* 2014; 83: 1437–1441.
46. Urcola JH, Hernández M & Vecino E. Three experimental glaucoma models in rats: comparison of the effects of intraocular pressure elevation on retinal ganglion cell size and death. *Exp Eye Res* 2006; 83: 429–437.
47. Rudzinski M, Wong T-P & Saragovi HU. Changes in retinal expression of neurotrophins and neurotrophin receptors induced by ocular hypertension. *J Neurobiol* 2004; 58: 341–354.
48. Song BJ & Caprioli J. New directions in the treatment of normal tension glaucoma. *Indian J Ophthalmol* 2014; 62: 529–537.
49. Osborne NN. Recent clinical findings with memantine should not mean that the idea of neuroprotection in glaucoma is abandoned. *Acta Ophthalmol* 2009; 87: 450–454.
50. Pascale A, Drago F & Govoni S. Protecting the retinal neurons from glaucoma: lowering ocular pressure is not enough. *Pharmacol Res* 2012; 66: 19–32.
51. Nucci C, Strouthidis NG & Khaw PT. Neuroprotection and other novel therapies for glaucoma. *Curr Opin Pharmacol* 2013; 13: 1–4.

52. Gupta N & Yücel YH. What changes can we expect in the brain of glaucoma patients? *Surv Ophthalmol* 2007; 52 (Suppl. 2): S122–S126.
53. Chang EE & Goldberg JL. Glaucoma 2.0: neuroprotection, neuroregeneration, neuroenhancement. *Ophthalmology* 2012; 119: 979–986.
54. Beaulieu C. The basis of anisotropic water diffusion in the nervous system – a technical review. *NMR Biomed* 2002; 15: 435–455.
55. Le Bihan D & Van Zijl P. From the diffusion coefficient to the diffusion tensor. *NMR Biomed* 2002; 15: 431–434.
56. Jbabdi S, Behrens TEJ & Smith SM. Crossing fibres in tract-based spatial statistics. *NeuroImage* 2010; 49: 249–256.
57. Chabert S, Molko N, Cointepas Y, Le Roux P & Le Bihan D. Diffusion tensor imaging of the human optic nerve using a non-CPMG fast spin echo sequence. *J Magn Reson Imaging* 2005; 22: 307–310.